


Transcriptome analysis reveals the molecular mechanisms of neonicotinoid acetamiprid in Leydig cells

Toxicology and Industrial Health
2025, Vol. 41(2) 61–72
© The Author(s) 2024
Article reuse guidelines:
sagepub.com/journals-permissions
DOI: 10.1177/07482337241300215
journals.sagepub.com/home/tih


Xun Liu¹, Ce Wang¹, Yue Ma², Linxiang Fu¹, Wanji Luo¹, Changjie Xu¹, Ying Tian³, Mingyue Ma² and Yaping Mao¹ 

Abstract

At present, the reproductive toxicology of neonicotinoids has received greater attention, however, its potential mechanisms are still not fully understood. Acetamiprid (ACE) is a new-generation neonicotinoid and has become a ubiquitous contaminant in the environment. This study aimed to investigate the toxic effects of ACE in TM3 Leydig cells based on transcriptome analysis. The viability and apoptosis of TM3 cells exposed to different concentrations of ACE were assessed by CCK8 and flow cytometry, respectively. After ACE exposure, transcriptome analysis was performed to screen differential expression genes (DEGs), followed by qPCR verification. Results showed that ACE exposure resulted in a time- and dose-dependent decrease in the viability of TM3 cells ($p < .05$). ACE also exerted a dose-dependent pro-apoptotic effect on TM3 cells. Results of RNA-seq showed that 1477 DEGs were obtained, of which 539 DEGs were up-regulated and 938 DEGs were down-regulated. GO and KEGG analyses of DEGs showed that DNA replication and cell cycle might be the key mechanisms for the cytotoxicity of ACE. qPCR results demonstrated that *Mdm2*, *Cdkn1a* (p21) and *Gadd45* were significantly increased, and *Pcna*, *Ccna2* (CycA), *Ccnb1* (CycB), *Ccne1* (CycE), and *Cdk1* were significantly decreased, indicating that ACE exposure might promote G1/S and G2/M cell cycle arrest. Additionally, FoxO, p53, and HIF-1 signaling pathways and ferroptosis might play important roles in ACE-induced reproductive toxicity. Collectively, this study provides new perspectives into the mechanism of ACE-induced reproductive toxicity and lays a theoretical foundation for the in-depth study of non-target toxicity mechanisms of neonicotinoid insecticides.

Keywords

Acetamiprid, reproductive toxicity, Leydig cells, transcriptome analysis, cell cycle

Received 9 May 2024; Revised 23 October 2024; Accepted 28 October 2024

Introduction

Neonicotinoids are a new group of broad-spectrum insecticides that are widely used around the world (Thompson et al., 2020; Zhang and Lu 2022). The first launched neonicotinoid was imidacloprid (IMI) in 1991, followed by nitenpyram (NIT) in 1995, acetamiprid (ACE) in 1996, thiamethoxam (THM) in 1997, thiacloprid (THD) in 1999, clothianidin (CLO), and dinotefuran (DIN) in 2002 (Mörtl et al., 2020). They are frequently employed to control insect pests in agriculture, horticulture, and on household pets (Han et al., 2018). Neonicotinoids are a class of potent agonists that selectively target the postsynaptic nicotinic acetylcholine

¹Department of Health Inspection and Quarantine, School of Public Health, Shenyang Medical College, Shenyang, China

²Department of Toxicology, School of Public Health, Shenyang Medical College, Shenyang, China

³MOE-Shanghai Key Laboratory of Children's Environmental Health, Xinhua Hospital, Shanghai Jiao Tong University School of Medicine, Shanghai, China

Corresponding author:

Yaping Mao, Department of Health Inspection and Quarantine, School of Public Health, Shenyang Medical College, No. 146, Huanghe North Street, Shenyang 110034, China.
Email: maoyaping195@163.com

receptors (nAChRs) in the central nervous system of insects. This highly specific mode of action causes neuromuscular paralysis and ultimately, death (Costas-Ferreira and Faro, 2021). Notably, neonicotinoids exhibit low affinity for vertebrate nAChRs, and they are rapidly metabolized with poor penetration of blood-brain barrier, rendering them less toxic to non-target organisms (Selvam and Srinivasan, 2019). Nonetheless, because of their low molecular weight, high water solubility, long half-life, and strong internal absorption, the extended use of neonicotinoids has led to their presence as pollutants in soil, surface water, and crops (Pietrzak et al., 2020; Zhang et al., 2018). Therefore, humans are continuously exposed to neonicotinoids via eating food, drinking water, inhalation, dermal contact, and indoor air contamination (Zhang and Lu, 2022). The Chinese total-diet studies demonstrated that most of the dietary samples were found to contain multiple neonicotinoids, IMI and ACE were found most frequently (Chen et al., 2020). Given the widespread presence of neonicotinoids in both food and the environment, the exposure risk of humans to neonicotinoids should not be overlooked.

In recent years, numerous studies have reported human exposure to neonicotinoids (Li and Kannan, 2020; Wrobel et al., 2022). Xu et al. (2021) reported data from 196 young adults in China and found that neonicotinoids and their metabolites were detected extensively in both urine (67%–91%) and blood (64%–97%) samples. Furthermore, exposure to neonicotinoids is affected by various factors, such as region, season, human age, and gender (Zhang et al., 2021). Nimako et al. (2021) reported that approximately 92% of the healthy volunteers were exposed to multiple neonicotinoids simultaneously in Africa, with N-demethyl-ACE (94.7%) having the highest detection rate, followed by IMI (70.7%). These increasing studies have shown that humans are widely exposed to neonicotinoids, indicating their potential health risks.

At present, with the increasing number of infertility cases, reproductive toxicology of neonicotinoids has received greater attention (Suwannarin et al., 2021). A cross-sectional study recruited 191 men from China reported that, in seminal plasma samples, N-desmethyl-ACE (98.4%), IMI-olefin (86.5%), and desmethyl-CLO (70.8%) were frequently detected (Wang et al., 2022). Studies on animals have also demonstrated that exposure to neonicotinoids can cause various male reproductive impairments, including damage to spermatogenesis, retardation of testicular development, and decreases in testosterone biosynthesis and semen quality (Arıcan et al., 2020;

Zou et al., 2023). However, the potential mechanisms of male reproductive toxicity induced by neonicotinoids are still not well understood.

ACE is a widely used and frequently detected neonicotinoid. Leydig cells can produce androgens that play key roles in spermatogenesis and male secondary sexual characteristics (Tang et al., 2022). Therefore, in the current study, ACE and TM3 Leydig cells were selected as the research objects, and the potential mechanisms whereby ACE induces reproductive toxicity were investigated by transcriptome sequencing technology, so as to provide a scientific foundation for the mechanism study of reproductive toxicity induced by neonicotinoid and the early prevention and intervention of reproductive diseases.

Materials and methods

Cell line culture

TM3 Leydig cells were obtained from Wuhan Procell Life Science and Technology Co., Ltd. (Wuhan, China). TM3 cells were grown in Dulbecco's Modified Eagle Medium (DMEM, Procell, China), which contained 4500 mg/L D-glucose. The culture medium was supplemented with 10% FBS (Gibco, USA) and 1% penicillin-streptomycin (Hyclone, USA). The cells were incubated at 37°C with 5% CO₂ in a humidified incubator.

ACE treatment of TM3 cells in vitro

ACE (MCE, CAS No. 135410-20-7, USA) with 99.88% purity was weighed and dissolved in dimethyl sulfoxide (DMSO, Sigma, USA). The ACE solution was further dissolved in DMEM to prepare the corresponding concentrations (final concentration of DMSO was 0.5%). TM3 cells were exposed to different concentrations of ACE when the cell density reached 60%–70% after passage. The concentration of DMSO was equal in the control group and ACE groups.

Cell viability assay

The viability of TM3 cells was assessed by Cell Counting Kit-8 (CCK8) (Vazyme, China). To select a proper concentration of ACE for further research, we constructed a concentration gradient of 1, 2, 4, 6, 8, 10, and 12 mmol/L ACE to measure the cell viability of TM3 cells after ACE exposure. TM3 cells were seeded into 96-well plates (5000 cells per well). At 24 h after passage, different concentrations of ACE were added

and then incubated for 24 h and 48 h, respectively. After washing twice with PBS, in each well, 100 μ L DMEM containing 10% CCK8 was added. The plates were incubated at 37°C for 30 min to 1 h (in the dark). The OD value was measured at a wavelength of 450 nm using a multifunctional microplate reader (Molecular Devices, USA).

Cell apoptosis assay

Flow cytometry was used to detect cell apoptosis rate. Annexin V-FITC/PI Apoptosis Detection Kit (Vazyme, China) was used to perform flow cytometry following the manufacturer's guide. TM3 cells were seeded into 6-well plates (1×10^5 cells per well). At 24 h after passage, cells were exposed to different concentrations of ACE for 24 h. TM3 cells were harvested using pancreatic enzymes without EDTA (Procell, China). After washing twice with precooled PBS, TM3 cells were resuspended in 100 μ L of $1 \times$ Binding Buffer. Then, 5 μ L of Annexin V-FITC and 5 μ L of PI Staining Solution were added, mixed, and incubated for 10 min at room temperature in the dark. After that, 400 μ L of $1 \times$ Binding Buffer were added. Cells were analyzed by flow cytometry within 1 h. All these experiments consisted of three independent biological replicates for quantification purposes.

RNA isolation and quality controls

Transcriptome analysis was performed in the control and 6 mmol/L ACE groups. Each group contained three replicates. Total RNA of the two groups was extracted using Trizol reagent (Vazyme, China) at 24 h after ACE exposure. The quantity, purity, and integrity of the total RNA were detected using NanoDrop NC200 (Thermo Scientific, USA), Bioanalyzer 2100 and RNA 6000 Nano Kit (Agilent, USA) with RNA integrity number (RIN) ≥ 6.5 .

RNA library construction and sequencing

The extracted RNA was enriched with oligo (dT) magnetic beads, then fragmented into shorter pieces (~ 300 bp) by ionic interruption. Subsequently, these RNA fragments were reverse-transcribed using the random hexamer primer to synthesize the initial cDNA strand, followed by the synthesis of the second cDNA strand. After construction of cDNA library, PCR amplification was performed to enrich library fragments, and library size about 450 bp was selected. The library's

quality was determined using Bioanalyzer 2100 (Agilent, USA), determining both the total and effective concentrations. Based on the required data amount and effective concentration of the library, different Index sequences libraries were proportionally blended. The pooled library was uniformly diluted to 2 nM, and a single-stranded library was constructed by alkali denaturation. Finally, paired-end sequencing was conducted using an Illumina sequencing platform, provided by Suzhou PANOMIX Biomedical Tech Co., LTD (Jiangsu, China). A graphical representation of the experimental process can be found in [Supplemental Figure S1](#).

Raw data processing and database comparison

The sequencing platform software transformed image files obtained from the samples into Raw Data of FASTQ. Each sample's Raw Data was individually analyzed for sample name, Q30, percentage of ambiguous bases, Q20 (%), and Q30 (%) ([Table 1](#)). Sequences with adapters at the 3' end were eliminated using Cutadapt, and reads with an average quality score lower than Q20 were discarded. Details of the data filtering can be found in [Table 2](#). Additional analyses included examining base mass, base content, and average quality distribution of the reads. The clean data were compared with the *Mus musculus* reference genome (GRCm38) using HISAT2 software (<https://ccb.jhu.edu/software/hisat2/index.shtml>).

Differentially expressed genes (DEGs) after ACE treatment in TM3 cells

HTSeq tallied the reads assigned to individual genes. The mRNA expression profile was normalized using fragments per kilo bases per million mapped reads (FPKM) to determine relative expression levels, with genes having FPKM > 1 being deemed as expressed. The correlation of gene expression levels between samples was assessed using the Pearson correlation coefficient. Principal Components Analysis (PCA) was conducted to analyze sample similarities.

DESeq was utilized for differential gene expression analysis between control and ACE groups, and the criteria for DEGs were $|\log_2 \text{foldchange}| > 1$ and $p < .05$. The “ggplot2” package in R was employed to visualize volcano plot. The “Circize” package in R was used to generate genome circos map. The “Pheatmap” package in R was used to draw heatmaps. The “topGO” package in R was used for Gene Ontology (GO) enrichment analysis of DEGs, and the “clusterProfiler” package in

Table 1. Basic information of raw data of RNA-Seq.

Sample	Reads no	Bases (bp)	Q30 (bp)	N (%)	Q20 (%)	Q30 (%)
CG_1	41,859,488	6,278,923,200	5,902,083,482	0.005205	97.73	93.99
CG_2	46,296,860	6,944,529,000	6,523,697,749	0.005132	97.73	93.94
CG_3	54,676,328	8,201,449,200	7,694,792,304	0.005157	97.66	93.82
ACE_1	44,309,226	6,646,383,900	6,257,387,575	0.005107	97.8	94.14
ACE_2	48,970,340	7,345,551,000	6,896,004,671	0.005219	97.67	93.88
ACE_3	44,191,872	6,628,780,800	6,203,926,908	0.005346	97.54	93.59

Note. TM3 cells were exposed to 0 mmol/L (CG: Control group) and 6 mmol/L ACE (Acetamidiprid), respectively; Q30 (bp): The total number of bases with base recognition rate above 99.9%; N (%): The percentage of ambiguous bases; Q20 (%): The percentage of bases with base recognition rate above 99%; Q30 (%): The percentage of bases with base-recognition rate above 99.9%.

Table 2. Details of the filtering of raw data.

Sample	Clean reads no	Clean data (bp)	Clean reads %	Clean data %
CG_1	38,471,682	5,770,752,300	91.9	91.9
CG_2	42,628,776	6,394,316,400	92.07	92.07
CG_3	49,880,144	7,482,021,600	91.22	91.22
ACE_1	40,561,618	6,084,242,700	91.54	91.54
ACE_2	45,128,504	6,769,275,600	92.15	92.15
ACE_3	40,568,222	6,085,233,300	91.8	91.8

Note. TM3 cells were exposed to 0 mmol/L (CG: control group) and 6 mmol/L ACE (Acetamidiprid), respectively; Clean Reads No.: Read number of high-quality sequences; Clean Data (bp): Number of bases of high-quality sequences; Clean Reads %: Percentage of high-quality sequence reads in sequenced reads; Clean Data %: Percentage of high-quality sequence in sequenced bases.

R was used for Kyoto Encyclopedia of Genes and Genomes (KEGG) enrichment analysis. Enrichment was considered significant if $p < .05$.

qPCR validation

Total RNA was extracted using Trizol reagent at 24 h after ACE exposure (0, 2, 4, 6 mmol/L). The concentration of the extracted RNA was detected using NanoDrop NC200. Subsequently, 1 μ g RNA underwent reverse transcription to generate cDNA using PrimeScriptTM RT-reagent Kit (TaKaRa Biotechnology, China). Further, qPCR analysis was carried out utilizing the TB Green[®] Premix Ex TaqTM (TaKaRa Biotechnology, China) by 7500 Real-time PCR System (Applied Biosystems Inc, USA). The primer sequences were listed in Table 3. *Gapdh* was utilized as an internal control. The relative expression of each gene was determined according to the $2^{-\Delta\Delta CT}$ method.

Statistical analysis

The mean \pm SD of three independent experiments are presented in the data. Statistical analysis was conducted using GraphPad Prism 9.0 software. Group differences were assessed with one-way ANOVA,

followed by Student's *t*-test, and statistical significance was defined as $p < .05$.

Results

Effects of ACE on the viability of TM3 cells

The viability of TM3 cells exposed to 0, 1, 2, 4, 6, 8, 10, and 12 mmol/L ACE for 24 h and 48 h, respectively, was detected using CCK8. Results indicated that ACE exposure reduced cell viability in a time- and dose-dependent manner ($p < .05$) (Figure 1A). The IC₅₀ at 24 h was calculated as 8.613 mmol/L. In subsequent experiments, 0, 2, 4, and 6 mmol/L ACE was used for testing purposes.

Pro-apoptotic effect of ACE on TM3 cells

Flow cytometry was performed to evaluate the pro-apoptotic effect of ACE treatment on TM3 cells for 24 h. The findings indicated that as the concentration of ACE increased, the rate of apoptosis in TM3 cells also gradually increased. A statistically significant difference was observed in the 4 and 6 mmol/L groups ($p < .05$) (Figures 1B and C). However, the apoptosis rate (14.8%) was less than the inhibiting rate of cell

Table 3. Primer sequences for qPCR.

Gene	Accession number	Sequence (5'→3')	Product length (bp)
<i>Mdm2</i>	NM_010786.4	Forward: AAGATGCGCGGGAAGTAGC Reverse: AGCACCCCTCGGTAGACACA	147
<i>Gadd45</i>	NM_007836.1	Forward: TGCTGCTACTGGAGAACGAC Reverse: TCCATGTAGCGACTTTCCCG	160
<i>Cdkn1a</i> (p21)	NM_007669.5	Forward: TCCAGACATTGAGAGCCACAG Reverse: CGAAGAGACAACGGCACACT	90
<i>Ccna2</i> (CycA)	NM_009828.3	Forward: GTCCTAACGCTCCCATCTCC Reverse: TCGGAAAGAGTGTGAGCCTC	72
<i>Ccnb1</i> (CycB)	NM_172301.3	Forward: GGCTAACGGAAGTTGTCGAA Reverse: AGGACACACAGTGAAGGATGT	122
<i>Ccne1</i> (CycE)	NM_007633.2	Forward: CCTTTCAGTCCGCTCCAGAA Reverse: GCTGACTGCTATCCTCGCTT	113
<i>Cdk1</i>	NM_007659.4	Forward: CACGGCGACTCAGAGATTGA Reverse: GGCTTCCACTTGGGAAAGGT	125
<i>Pcna</i>	NM_011045.2	Forward: GAAGTTTTCTGCAAGTGGAGAG Reverse: CAGGCTCATTCTCTATGGT	107
<i>Gapdh</i>	NM_001289726.2	Forward: TGTGTCCGTCGTGGATCTGA Reverse: CCTGCTTCACCACCTTCTTGAT	77

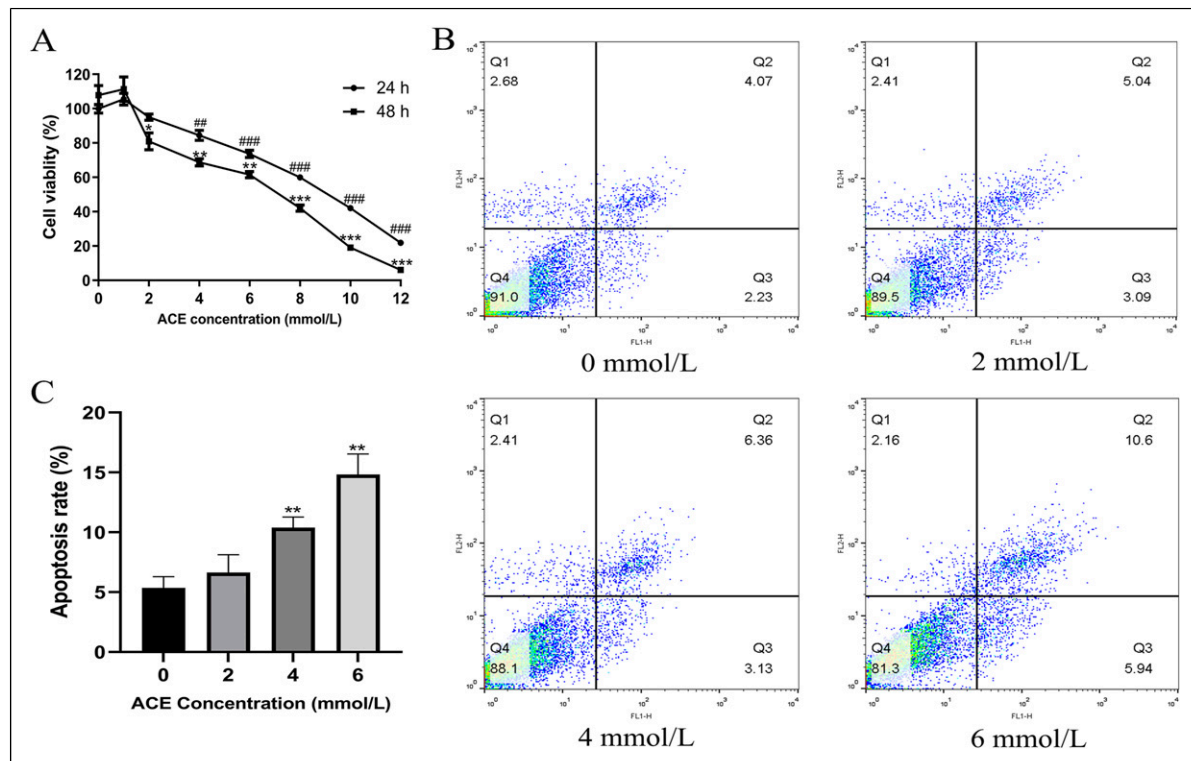


Figure 1. Cytotoxic effects of ACE on TM3 cells. (A) TM3 cells were exposed to different concentrations of ACE for 24 and 48 h, and cell viability was detected using CCK-8. Data were expressed as mean \pm SD ($n = 6$); ### $p < .01$, #### $p < .001$, compared with 0 mmol/L ACE group; * $p < .05$, ** $p < .01$, *** $p < .001$, compared with 24 h group. (B) TM3 cells were exposed to 0, 2, 4, 6 mmol/L ACE for 24 h, and apoptosis rate was detected using flow cytometry. (C) The statistic of apoptosis rate of TM3 cells. Data were expressed as mean \pm SD ($n = 3$); ** $p < .01$, compared with 0 mmol/L ACE group.

viability (26.3%) in the 6 mmol/L group. Therefore, we speculated that there were other key mechanisms underlying the toxic effects of ACE on TM3 cells.

Transcriptome analysis of TM3 cells exposed to ACE

To evaluate potential mechanisms of TM3 cells damage induced by ACE exposure, mRNA sequencing of TM3 cells exposed to 0 and 6 mmol/L ACE was performed. The clean data were compared with the *Mus musculus* reference genome, and the fundamental information of sequence alignment is displayed in Table 4. Pearson correlation coefficient (Figure 2A) and PCA (Figure 2B) demonstrated excellent internal consistency. Based on $|\log_2\text{Fold-Change}| > 1$ and $p < .05$, there were 1477 DEGs with 539 DEGs showing up-regulation and 938 DEGs down-regulation (Supplemental Table S1 and S2). The distribution of DEGs between control and ACE groups is presented in the volcano plot (Figure 2C). Genome circos was generated to map DEGs (Figure 2D). Clustering analysis of DEGs presented as a clustering heatmap showed that the differences between the expression patterns of the two groups were significant (Figure 2E).

GO and KEGG enrichment analyses of DEGs

Towards an in-depth view of DEGs in the TM3 cells exposed to ACE, enrichment analyses of GO and KEGG were conducted. DEGs were organized based on the GO terms classification, which included cellular component (CC), molecular function (MF), and biological process (BP). In each GO category, the top 10 GO terms were shown in Figure 3A. The CC category

was significantly related to chromosomal region, kinetochore, nuclear chromosome, etc. The MF category was significantly related to protein binding, catalytic activity, DNA-dependent ATPase activity, DNA helicase activity, nucleotide binding, and ATP binding. The BP category was significantly related to cell cycle process, DNA replication, DNA metabolic process, cell division, chromosome segregation, and organization. The results of GO enrichment analysis indicated that ACE significantly affected DNA replication and cell cycle process. Furtherly, KEGG enrichment analysis of DEGs was performed and the top 30 terms were shown in Figure 3B. The KEGG pathways were significantly related to DNA replication, cell cycle, mismatch repair, homologous recombination, and base excision repair. ACE treatment also affected the p53 signaling pathway, HIF-1 signaling pathway, ferroptosis, FoxO signaling pathway and ABC transporters. DEGs were related to platinum drug resistance, microRNAs in cancer, and pathways in cancer. Pyrimidine metabolism, glutathione metabolism, tryptophan metabolism, drug metabolism, and cysteine and methionine metabolism were also affected by ACE treatment.

Validation of DEGs related to cell cycle pathway using qPCR

In light of the results of GO and enrichment analyses, cell cycle pathway was one of the key mechanisms of ACE-induced TM3 cell damage, which is depicted in Figure 4. Therefore, cell cycle-related genes of TM3 cells exposed to 0, 2, 4, and 6 mmol/L ACE for 24 h were validated by qPCR. Figure 5 presents the comparison of mRNA levels in different ACE groups with the control group. It was found that the mRNA levels

Table 4. The fundamental information of RNA-Seq map.

Sample	Clean_Reads	Total_Mapped	Multiple_Mapped	Uniquely_Mapped
CG_1	38,471,682	36935378 (96.01%)	2419715 (6.55%)	34515663 (93.45%)
CG_2	42,628,776	40949809 (96.06%)	2717558 (6.64%)	38232251 (93.36%)
CG_3	49,880,144	47818961 (95.87%)	3069210 (6.42%)	44749751 (93.58%)
ACE_1	40,561,618	38919689 (95.95%)	2502850 (6.43%)	36416839 (93.57%)
ACE_2	45,128,504	43428743 (96.23%)	3002615 (6.91%)	40426128 (93.09%)
ACE_3	40,568,222	38942404 (95.99%)	2615186 (6.72%)	36327218 (93.28%)

Note. TM3 cells were exposed to 0 mmol/L (CG: Control group) and 6 mmol/L ACE (Acetamidiprid), respectively; Clean Reads: The total number of sequences used for alignment; Total Mapped: The Total number of sequences aligned to the reference genome, the percentage is total Mapped/Clean Reads; Multiple Mapped: The total number of sequences aligned to multiple positions, the percentage is Multiple Mapped/Total Mapped; Uniquely Mapped: The total number of sequences aligned to a position only, the percentage is Uniquely Mapped/Total Mapped.

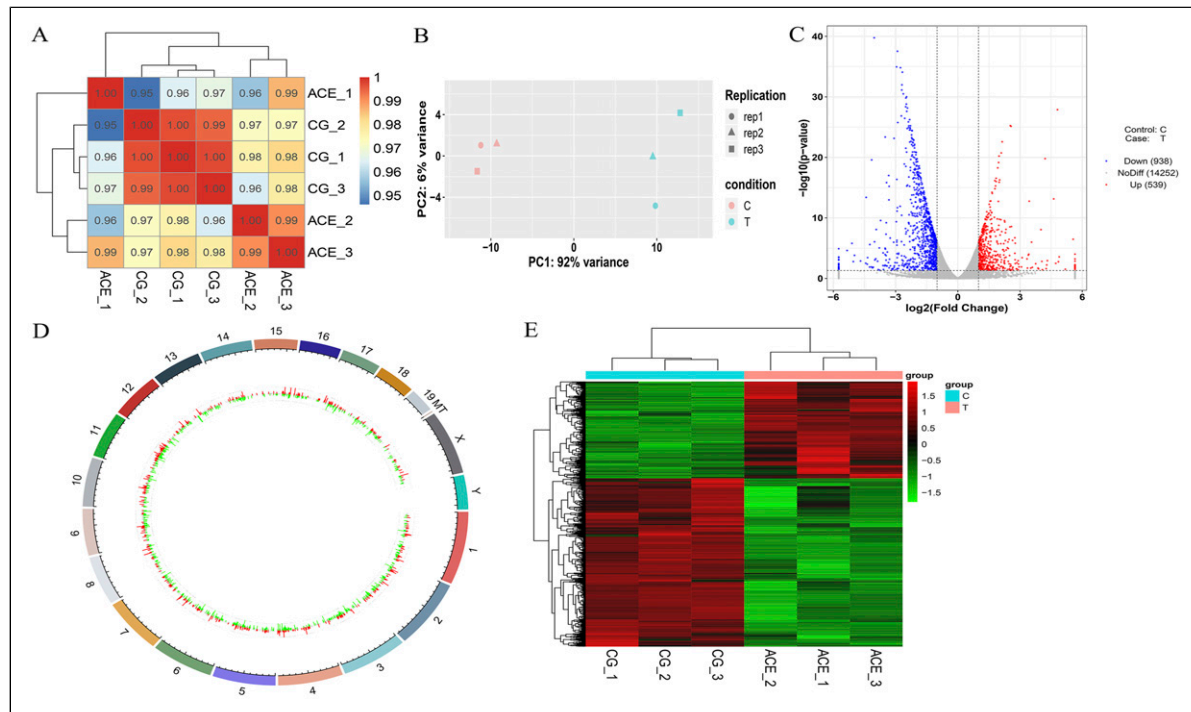


Figure 2. ACE exposure altered mRNA expression in TM3 cells. (A) Pearson correlation analysis; (B) Principal component analysis (PCA); (C) Volcano plot of DEGs between 0 and 6 mmol/L ACE groups; (D) Genome circle showed the genome-wide distribution of mRNAs; (E) Heatmap analysis of DEGs.

of *Mdm2*, *Cdkn1a* (p21), and *Gadd45* were significantly increased in all ACE groups ($p < .05$). Conversely, the mRNA levels of *Pcna*, *Ccna2* (CycA), *Ccnb1* (CycB), *Ccne1* (CycE), and *Cdk1* were significantly decreased in the 6-mmol/L ACE group. These changes in gene expression were in line with the transcriptomic data. In addition to the cell cycle pathway, these genes were also involved in platinum drug resistance, the p53 signaling pathway, microRNAs in cancer, pathways in cancer, the FoxO signaling pathway, oocyte meiosis, and cellular senescence.

Discussion

Growing evidence from clinical and epidemiological studies has demonstrated that an increase in male reproductive disorders is becoming more prevalent, with environmental exposures resulting from contemporary lifestyle, rather than genetic factors, being the primary contributors (Skakkebaek et al., 2016). Notably, pesticides are thought to act as endocrine disruptors and their extensive use is an important risk factor responsible for reproductive problems (Chiang et al., 2017). More recent studies have confirmed that ACE, one of the most

frequently detected neonicotinoid insecticides, can cause toxicity to the male reproductive system, including decreased sperm count, viability, motility and morphology, reduced testosterone and gonadotropin-releasing hormones (GnRH), decreased number of spermatogenic germ cells and spermatozoa, and necrosis of spermatocytes (Arican et al., 2020; Sevim et al., 2023; Toghan et al., 2022). As yet, apart from oxidative stress (Arican et al., 2020; El-Hak et al., 2022), little is known about the mechanism of ACE-induced reproductive toxicity. Therefore, we conducted RNA-seq and deep transcriptomic analysis to delve deeper into understanding the potential toxicity mechanism of ACE on Leydig cells.

As far as we know, there has been no prior research reporting the cytotoxic impact of ACE on Leydig cells in vitro. Therefore, we determined the effects of ACE on the viability and apoptosis of TM3 Leydig cells. The findings indicated that ACE exposure markedly reduced cell viability and increased apoptosis rate in TM3 cells. In vivo studies, transmission electron microscopy (TEM) examination showed hydropic degeneration, electron-dense lipid vacuoles, chromatinolysis, and mitochondrial membrane damage in the Leydig cell cytoplasm after ACE exposure (Kong et al., 2017; Zayman et al., 2022). In vitro study,

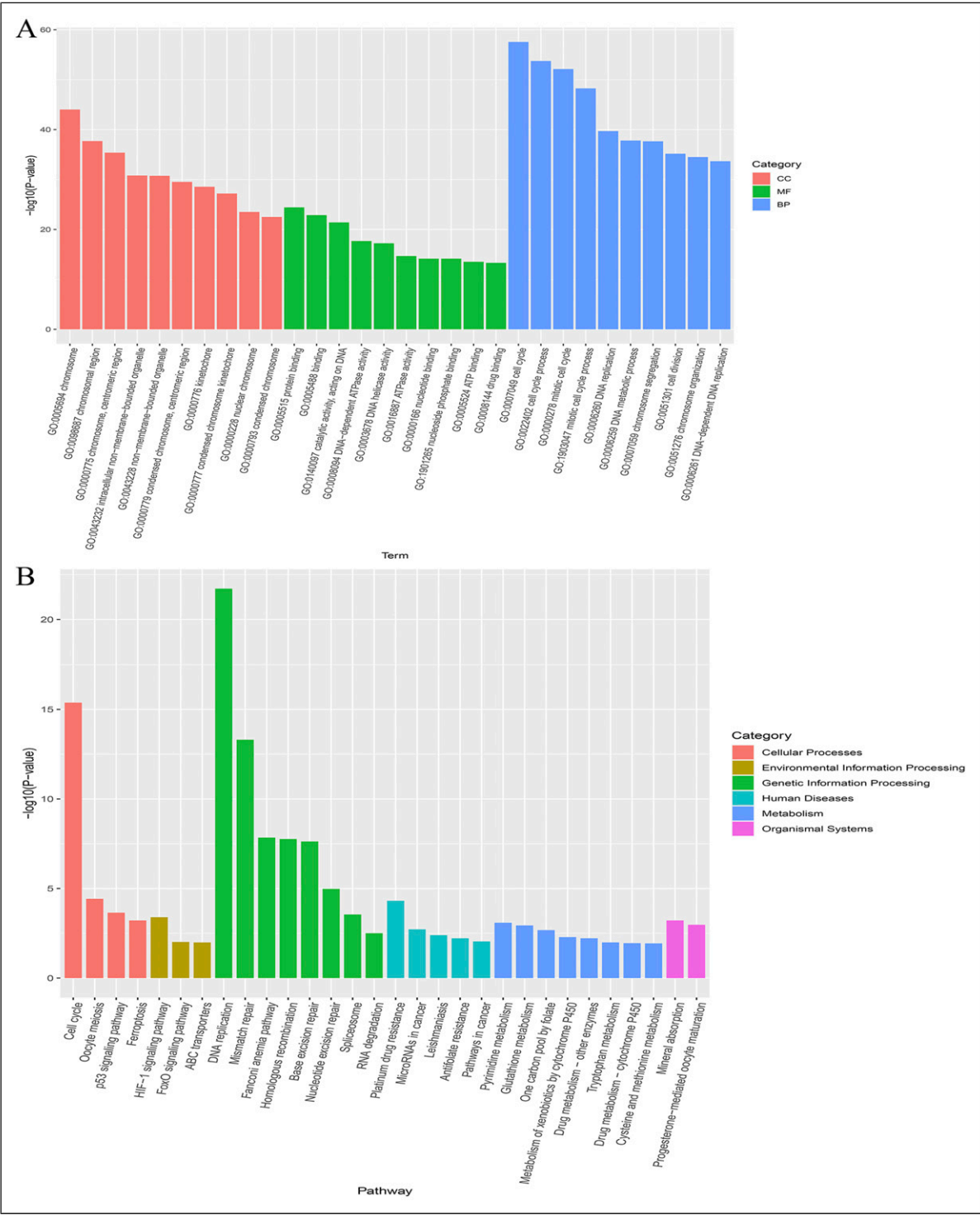
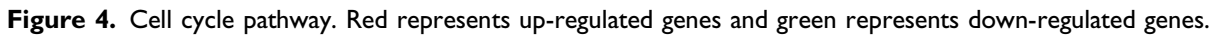


Figure 3. GO and KEGG enrichment analyses of DEGs. (A) Top 10 terms of GO enrichment analysis. CC: cellular component; MF: molecular function; BP: biological process. (B) KEGG pathway analysis of DEGs.

the cytotoxicity of IMI observed in LC-540, a rat Leydig cell line, could be due to cytoplasmic vacuoles, damage to mitochondria, autophagic vacuoles, and disruption of cytoskeletal protein. Therefore, the

cytotoxicity of ACE may also relate to mitochondrial damage (Ibrahim et al., 2023). Moreover, besides promoting apoptosis, other important mechanisms may exist for the cytotoxic effects of ACE.



downstream effectors, such as p21 and growth arrest and DNA damage-induced Gene 45 (GADD45). Entry into the proliferative cycle is regulated by Cyclin/Cyclin-dependent kinases (CDKs), with p21 (cyclin-dependent kinase inhibitor) binding to Cyclin/CDKs complexes to form a trimeric and inhibit CDK activity in the G1 phase, leading to G1 phase arrest (Swadling et al., 2022). The interaction of GADD45 with proliferating cell nuclear antigen (PCNA) also plays a crucial role in inhibiting DNA synthesis and preventing cells from progressing into S phase (Vairapandi et al., 2000). Additionally, GADD45 is involved in the G2/M checkpoint, its overexpression can result in a decrease of nuclear CycB protein and a change in sub-cellular localization of CycB, which is a critical step in the G2/M cell cycle arrest induced by GADD45 (Jin et al., 2002). Collectively, the increased *Mdm2*, *Cdkn1a* (p21), and *Gadd45* and the decreased *Pcna*, *Ccna2* (CycA), *Ccnb1* (CycB), and *Ccne1* (CycE) indicate that further investigation is required to explore the specific

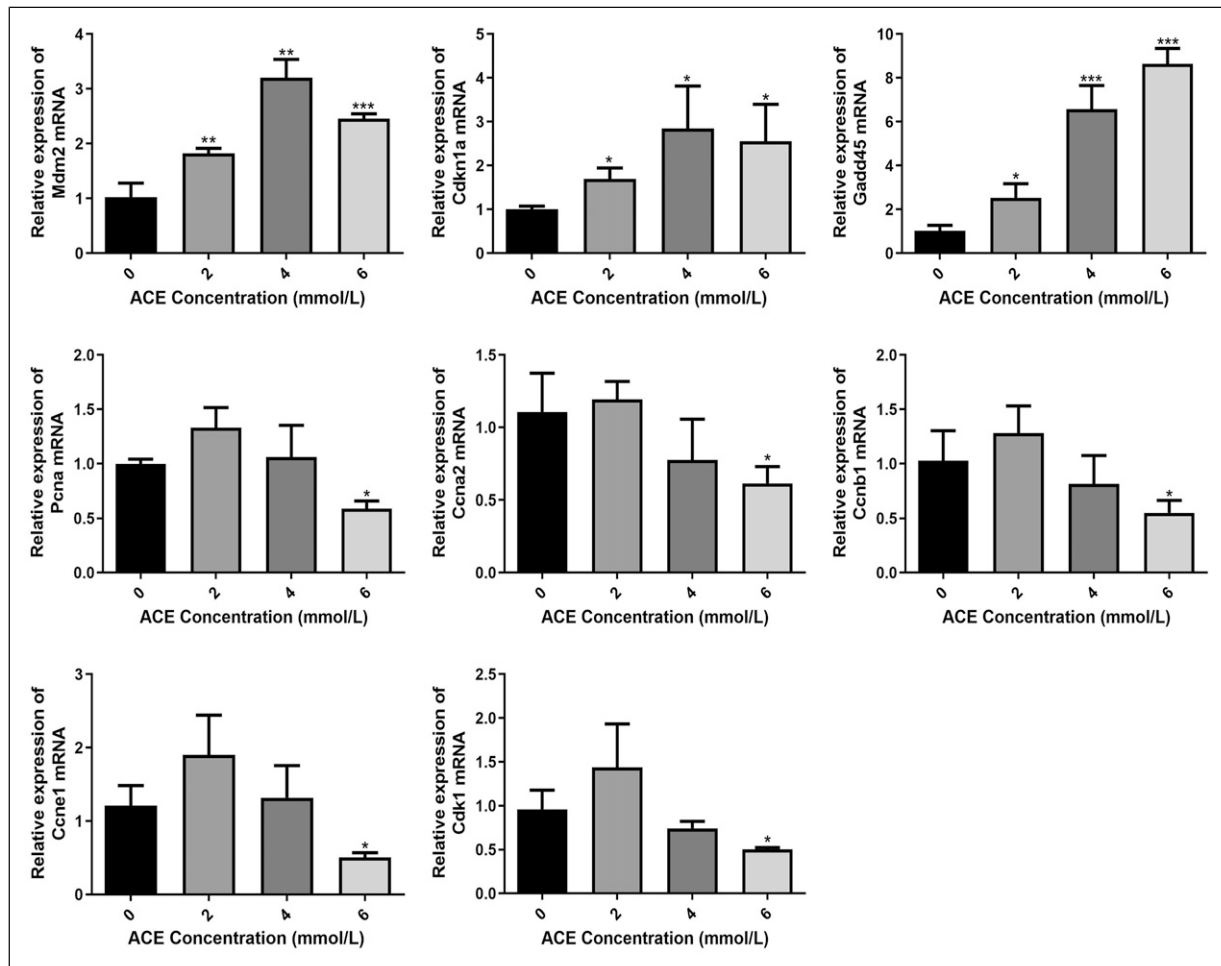


Figure 5. Verification of cell cycle-related DEGs by qPCR. Data were expressed as mean \pm SD ($n = 3$); * $p < .05$, ** $p < .01$, *** $p < .001$, compared with 0 mmol/L ACE group.

molecular mechanisms underlying the potential cytotoxic effects of ACE in inducing G1/S and G2/M cell cycle arrest.

KEGG enrichment analysis indicated the effects of ACE on the p53 signaling pathway, HIF-1 signaling pathway, ferroptosis, and FoxO signaling pathway. Meanwhile, the above cell cycle-related genes are also involved in the p53 and FoxO signaling pathways. Overlapping functions of FoxO and p53 in cell-cycle regulation and tumor suppression are demonstrated, and they share several downstream target genes such as GADD45 and p21 (Bourgeois and Madl, 2018). Xie et al. (2022) demonstrated that activation of the p53 signaling pathway plays a crucial role in thiocloprid-induced hepatotoxicity.

Ferroptosis is a form of regulated cell death that depends on iron levels and is triggered when testicular tissue is exposed to certain risk factors, including endocrine disrupting chemicals, cadmium, and smoking (Su et al.,

2022). Ferroptosis can cause the accumulation of reactive oxygen species (ROS) that damage sperm by targeting the cell membrane and DNA, thereby causing male reproductive dysfunction (Liu et al., 2022). Wu et al. (2022) reported that MEHP exposure resulted in accumulation and stabilization of HIF-1 α , followed by its nuclear translocation to form a HIF-1 α /Hmox1 complex in Leydig and Sertoli cells, and a knockout of *Hif-1 α* was found to rescue MEHP-induced ferroptosis, indicating the important role of HIF-1 α signaling pathway in ferroptosis. Overall, our results suggest that p53, FoxO, HIF-1 signaling pathways, and ferroptosis may be key mechanisms of ACE-induced reproductive toxicity.

In conclusion, this study investigated the molecular mechanism of ACE toxicity on Leydig cells using transcriptome sequencing analysis. ACE exposure can significantly reduce cell viability and promote apoptosis of Leydig cells. Moreover, it may also promote G1/S and G2/M cell cycle arrest. Importantly, crosstalk

between FoxO and p53 signaling pathways may be critical for cell-cycle regulation. Additionally, HIF-1 signaling pathways and ferroptosis may play a crucial role in ACE-induced reproductive toxicity involved in DNA damage and oxidative stress. One limitation of this study is that in vivo ACE exposure was not performed. Therefore, these key mechanisms will be further verified by in vivo and in vitro studies. Overall, this study provided novel insights into the mechanism of ACE-induced reproductive toxicity and lays a theoretical foundation for the in-depth study of non-target toxicity mechanisms of neonicotinoid insecticides.

Declaration of conflicting interests

The author(s) declared no potential conflicts of interest with respect to the research, authorship, and/or publication of this article.

Funding

The author(s) disclosed receipt of the following financial support for the research, authorship, and/or publication of this article: This work was supported by the Project of Innovation Training Plan for College Students of Shenyang Medical College (grant number X202310164014), the Science and Technology Research Project of Education Department of Liaoning Province (grant number LJKMZ20221782), the Science and Technology Program of Liaoning Province (grant number 2023-MS-327), and the Open Project of MOE-Shanghai Key Laboratory of Children's Environmental Health (grant number 202002).

ORCID iD

Yaping Mao  <https://orcid.org/0009-0006-2690-136X>

Data availability statement

All data analyzed during this study are either included in this article or are available from the corresponding author upon request.

Supplemental Material

Supplemental material for this article is available online.

References

- Arıcan EY, Gökçeoğlu Kayalı D, Ulus Karaca B, et al. (2020) Reproductive effects of subchronic exposure to acetamiprid in male rats. *Scientific Reports* 10: 8985.
- Bourgeois B and Madl T (2018) Regulation of cellular senescence via the FOXO4-p53 axis. *FEBS Letters* 592: 2083–2097.
- Chen D, Zhang Y, Lv B, et al. (2020) Dietary exposure to neonicotinoid insecticides and health risks in the Chinese general population through two consecutive total diet studies. *Environment International* 135: 105399.
- Chiang C, Mahalingam S and Flaws JA (2017) Environmental contaminants affecting fertility and somatic health. *Seminars in Reproductive Medicine* 35: 241–249.
- Costas-Ferreira C and Faro LRF (2021) Neurotoxic effects of neonicotinoids on mammals: what is there beyond the activation of nicotinic acetylcholine receptors? a systematic review. *International Journal of Molecular Sciences* 22: 8413.
- El-Hak HNG, Al-Eisa RA, Ryad L, et al. (2022) Mechanisms and histopathological impacts of acetamiprid and azoxystrobin in male rats. *Environmental Science and Pollution Research International* 29: 43114–43125.
- Galdíková M, Holečková B, Šivíková K, et al. (2019) Evaluating the genotoxic damage in bovine whole blood cells in vitro after exposure to thiacloprid. *Toxicology in Vitro* 61: 104616.
- Han W, Tian Y and Shen X (2018) Human exposure to neonicotinoid insecticides and the evaluation of their potential toxicity: an overview. *Chemosphere* 192: 59–65.
- Ibrahim M, Ferreira G, Venter EA, et al. (2023) Cytotoxicity, morphological and ultrastructural effects induced by the neonicotinoid pesticide, imidacloprid, using a rat leydig cell line (LC-540). *Environmental Toxicology and Pharmacology* 104: 104310.
- Jin S, Tong T, Fan W, et al. (2002) GADD45-induced cell cycle G2-M arrest associates with altered subcellular distribution of cyclin B1 and is independent of p38 kinase activity. *Oncogene* 21: 8696–8704.
- Kong D, Zhang J, Hou X, et al. (2017) Acetamiprid inhibits testosterone synthesis by affecting the mitochondrial function and cytoplasmic adenosine triphosphate production in rat leydig cells. *Biology of Reproduction* 96: 254–265.
- Li AJ and Kannan K (2020) Profiles of urinary neonicotinoids and dialkylphosphates in populations in nine countries. *Environment International* 145: 106120.
- Liu Y, Cao X, He C, et al. (2022) Effects of ferroptosis on male reproduction. *International Journal of Molecular Sciences* 23: 7139.
- Mörtl M, Vehovszky Á, Klátyik S, et al. (2020) Neonicotinoids: spreading, translocation and aquatic toxicity. *International Journal of Environmental Research and Public Health* 17: 2006.
- Nimako C, Ikenaka Y, Akoto O, et al. (2021) Human exposures to neonicotinoids in Kumasi, Ghana. *Environmental Toxicology and Chemistry* 40: 2306–2318.
- Pietrzak D, Kania J, Kmiecik E, et al. (2020) Fate of selected neonicotinoid insecticides in soil-water systems: current state of the art and knowledge gaps. *Chemosphere* 255: 126981.
- Selvam V and Srinivasan S (2019) Neonicotinoid poisoning and management. *Indian Journal of Critical Care Medicine* 23: S260–S262.

- Sevim Ç, Akpınar E, Aksu EH, et al. (2023) Reproductive effects of *S. boulardii* on sub-chronic acetamiprid and imidacloprid toxicity in male rats. *Toxics* 11: 170.
- Skakkebaek NE, Rajpert-De Meyts E, Buck Louis GM, et al. (2016) Male reproductive disorders and fertility trends: influences of environment and genetic susceptibility. *Physiological Reviews* 96: 55–97.
- Su Y, Liu Z, Xie K, et al. (2022) Ferroptosis: a novel type of cell death in male reproduction. *Genes* 14: 43.
- Suwannarin N, Prapamontol T, Isobe T, et al. (2021) Exposure to organophosphate and neonicotinoid insecticides and its association with steroid hormones among male reproductive-age farmworkers in northern Thailand. *International Journal of Environmental Research and Public Health* 18: 5599.
- Swadling JB, Warnecke T, Morris KL, et al. (2022) Conserved Cdk inhibitors show unique structural responses to tyrosine phosphorylation. *Biophysical Journal* 121: 2312–2329.
- Tang Q, Zhang Y, Yue L, et al. (2022) Ssc-miR-21-5p and Ssc-miR-615 regulates the proliferation and apoptosis of leydig cells by targeting SOX5. *Cells* 11: 2253.
- Thompson DA, Lehmler HJ, Kolpin DW, et al. (2020) A critical review on the potential impacts of neonicotinoid insecticide use: current knowledge of environmental fate, toxicity, and implications for human health. *Environmental Science. Processes & Impacts* 22: 1315–1346.
- Toghan R, Amin YA, Ali RA, et al. (2022) Protective effects of folic acid against reproductive, hematological, hepatic, and renal toxicity induced by Acetamiprid in male Albino rats. *Toxicology* 469: 153115.
- Vairapandi M, Azam N, Balliet AG, et al. (2000) Characterization of MyD118, Gadd45, and proliferating cell nuclear antigen (PCNA) interacting domains. PCNA impedes MyD118 AND Gadd45-mediated negative growth control. *Journal of Biological Chemistry* 275: 16810–16819.
- Wang A, Wan Y, Zhou L, et al. (2022) Neonicotinoid insecticide metabolites in seminal plasma: associations with semen quality. *The Science of the Total Environment* 811: 151407.
- Wrobel SA, Bury D, Hayen H, et al. (2022) Human metabolism and urinary excretion of seven neonicotinoids and neonicotinoid-like compounds after controlled oral dosages. *Archives of Toxicology* 96(1): 121–134.
- Wu Y, Wang J, Zhao T, et al. (2022) Di-(2-ethylhexyl) phthalate exposure leads to ferroptosis via the HIF-1 α /HO-1 signaling pathway in mouse testes. *Journal of Hazardous Materials* 426: 127807.
- Xie Z, Lu G, Zhou R, et al. (2022) Thiacloprid-induced hepatotoxicity in zebrafish: activation of the extrinsic and intrinsic apoptosis pathways regulated by p53 signaling pathway. *Aquatic Toxicology* 246: 106147.
- Xu M, Zhang Z, Li Z, et al. (2021) Profiles of neonicotinoid insecticides and characteristic metabolites in paired urine and blood samples: partitioning between urine and blood and implications for human exposure. *The Science of the Total Environment* 773: 145582.
- Zayman E, Gül M, Erdemli ME, et al. (2022) Biochemical and histopathological investigation of the protective effects of melatonin and vitamin E against the damage caused by acetamiprid in Balb-c mouse testicles at light and electron microscopic level. *Environmental Science and Pollution Research International* 29: 47571–47584.
- Zhang D and Lu S (2022) Human exposure to neonicotinoids and the associated health risks: a review. *Environment International* 163: 107201.
- Zhang Q, Li Z, Chang CH, et al. (2018) Potential human exposures to neonicotinoid insecticides: a review. *Environmental Pollution* 236: 71–81.
- Zhang C, Yi X, Xie L, et al. (2021) Contamination of drinking water by neonicotinoid insecticides in China: human exposure potential through drinking water consumption and percutaneous penetration. *Environment International* 156: 106650.
- Zhao Y, Cai J, Shi K, et al. (2021) Germacrone induces lung cancer cell apoptosis and cell cycle arrest via the Akt/MDM2/p53 signaling pathway. *Molecular Medicine Reports* 23: 452.
- Zou Y, Zhang L, Yue M, et al. (2023) Reproductive effects of pubertal exposure to neonicotinoid thiacloprid in immature male mice. *Toxicology and Applied Pharmacology* 474: 116629.